

Review

Recent Trends in Electrochemical Detection of NH₃, H₂S and NO_x Gases

Muzamil Ahmad Khan¹, Farah Qazi¹, Zakir Hussain^{1,*}, Muhammad Umair Idrees¹, Shahid Soomro², Saeeda Soomro²

¹ School of Chemical and Materials Engineering (SCME), National University of Sciences & Technology (NUST), Sector H-12, 44000 Islamabad, Pakistan
Tel.: 0092 51 9085 5205; Fax. 0092 51 9085 5002

² Bremer Pharma GmbH, Werkstr. 42, 34414 Warburg, Germany

*E-mail: zakir.hussain@scme.nust.edu.pk

Received: 6 December 2016 / Accepted: 27 January 2017 / Published: 12 February 2017

Due to the incorporation of nanomaterials, electrochemical sensors are emerging as a crucial tool for environmental monitoring as they provide flexibility in analysis and monitoring of environmental pollutants away from the sophisticated labs. Among various environmental pollutants, analysis and monitoring of toxic gases is essentially required. In this review, some recent trends have been reviewed and discussed regarding the application of nanomaterials for electrochemical detection of H₂S, NO_x, and NH₃. Precisely, work carried out during the last decade has been studied and the basic quality assurance parameters of these electrochemical gas sensors in terms of operational conditions (sensitivity, selectivity, limit of detection and response time) have been evaluated and presented. Some typical responses data of the developed devices have been discussed. Among various improvements of analytical performance, these nanomaterials based electrochemical systems have shown increased sensitivity and decreased detection limits.

Keywords: electrochemical gas sensors, toxic gases, limit of detection, response time, sensing parameters, nanomaterials

1. INTRODUCTION

Accurate monitoring of toxic gases and detection of environmental pollutants has become a primary concern due to rapid progress in industrialization during the recent years. In order to reduce pollution caused by expansion of manufacturing industries operating from advance countries to developing countries, strict regulations have to be imposed [1]. In this regard, designing of robust, low

cost and portable sensors is an essential requirement and progressive research is being conducted in order to develop new ranges of chemical sensors with enhanced sensitivity.

Major toxic gases in the air may include carbon monoxide (CO), nitrogen oxides (NO_x), Sulfur dioxide (SO₂), ammonia (NH₃), and hydrogen sulfide (H₂S) [2-7]. CO is colorless and odorless gas with density slightly less than that of the air. This gas is extremely dangerous to hemoglobin if consumed at above 35ppm concentration. CO is mostly produced as a byproduct when burning of organic compounds take place. Similarly, NH₃ is a colorless gas with pungent smell. The main source of ammonia generation is agricultural activity when soil is fertilized with ammonium ion [5]. Combustion in the chemical plant is another source of production of NH₃ gas. NH₃ gas at 300ppm causes immediate danger to health and hence it is extremely essential to know its threshold limit value [8, 9]. SO₂ gas is usually released when fossils fuels (coal and heavy oils) are burned. It has pungent, irritating smell and causes strong irritation to eyes with coughing and chest tightness. The current OSH standard is 5ppm average over an eight hour work shift[10]. Similarly, mobile and stationary combustion sources are responsible for emission of NO_x gas. NO rapidly reacts with ozone in the atmosphere to form NO₂ leading to global warming. H₂S gas has stinking smell like that of rotten eggs. It commonly occurs naturally or is produced through certain industrial activities. If inhaled, H₂S is rapidly absorbed by lungs and its exposure at higher concentrations severely affects respiratory system that could lead to unconsciousness or even death [11]. These gases have adverse effects on the humans and to the environment.

Over the last decades, instruments based on gas detection have been introduced to monitor the working atmospheres of these gases. Gas monitoring offer broad range of applications and play an important role in many areas, such as personal safety, medical diagnosis, pollutant detection and transportation industries [12]. For the quantitative analysis of toxic gases, such as mentioned above, various physical and chemical principles are involved [13]. Different types of gas sensors such as photo ionization sensors [13-15], IR sensors [16], fluorescent sensors [17-19], metal oxide semiconductor [20], catalytic gas sensors [21] and electrochemical gas sensors [22] are used for the detection of these gases. Several sensing platforms used in laboratory to monitor toxic gases may include pellistores, optical sensors and semiconductor gas sensors. Pellistores change resistance in the presence of gas and consists of catalyst loaded ceramic pellets. Such sensing platform exhibits higher sensitivity however, faces zero drift at ppm concentration [23]. The problem of zero drift and cross sensitivity was observed in semiconductor gas sensors as well [24]. Optical sensors could achieve higher sensitivity, selectivity and stability than non-optical methods but due to miniaturization and relatively high cost, their applications on gas sensors are seriously restricted [25]. In comparison to these sensing platforms, electrochemical gas sensors have significant advantages for quantifying and detecting hazardous gases such as NH₃, H₂S, NO_x etc. [26]. These sensors are relatively specific to individual gas with sensitivity at ppm and ppb levels [27]. Few of the key attributes of the electrochemical sensors may include room temperature operating conditions, compact size, low cost, high portability and better selectivity [28]. Electrochemical sensors are extensively being employed in various applications, indicating the scope and potential of this area (Figure 1).

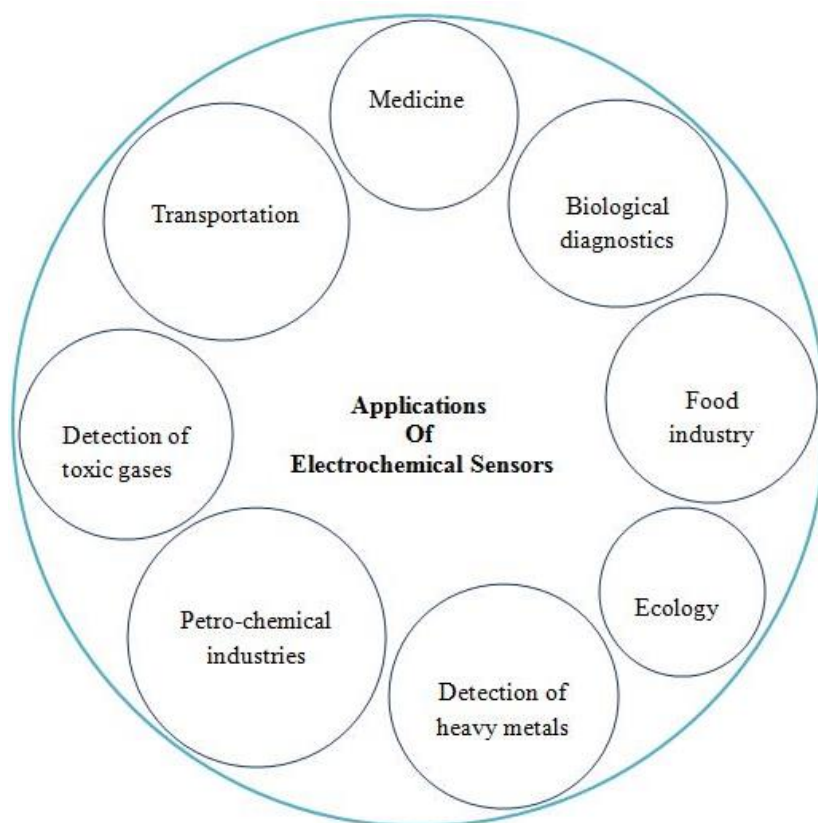


Figure 1. Schematic diagram showing applications scope of electrochemical sensors

The basic principle of an electrochemical sensor is that it detects the electron that is transferred during an electrochemical reaction [29]. Basically, the principal electrochemical gas sensing component is an electrochemical cell, where electrolyte is in contact with its surrounding through the electrodes. A typical electrochemical gas sensor (Figure 2) consist of a gas permeable membrane and three electrodes namely, (i) sensing electrode (SE) or working electrode (WE), (ii) counter electrode (CE), and (iii) reference electrode (RE).

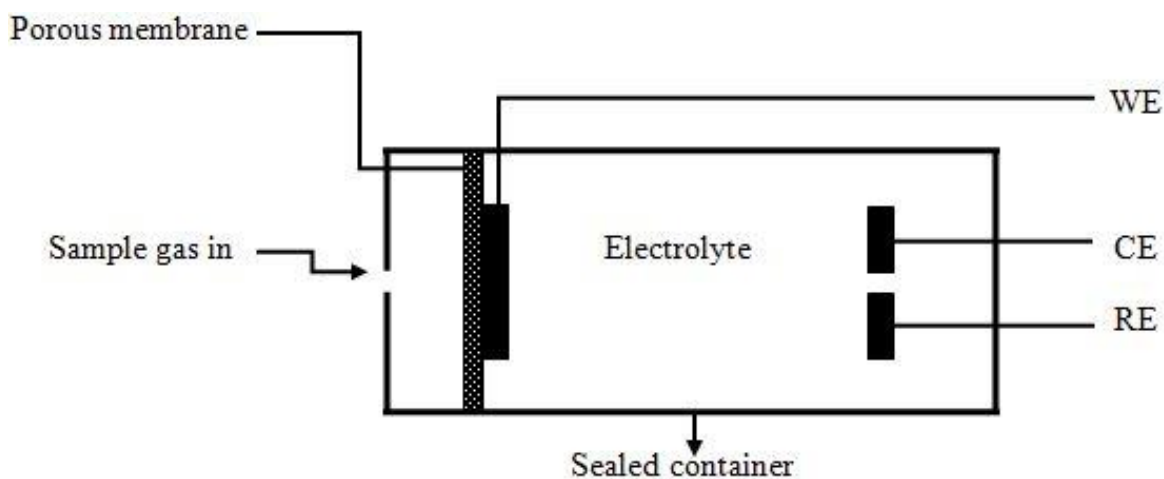


Figure 2. Schematic diagram of a typical electrochemical gas sensor

In an electrochemical gas sensor, the gas of interest diffuses through a membrane followed by its interaction at the surface of the sensing electrode resulting in either an oxidation or reduction mechanism (Figure 3). This results in a current flow between the sensing and counter electrode which produces an appreciable electrical signal. The generated electric signals are extracted from counter electrode and interpreted as the current changes with gas concentration. For sensing, the sensing electrode potential must be constant but due to continuous reaction taking place at sensing electrode surface, this potential varies resulting in degradation of sensor performance. To avoid this and improve the sensor performance, usually a reference electrode is placed in between sensing and counter electrode. No external current is associated with reference electrode [30].

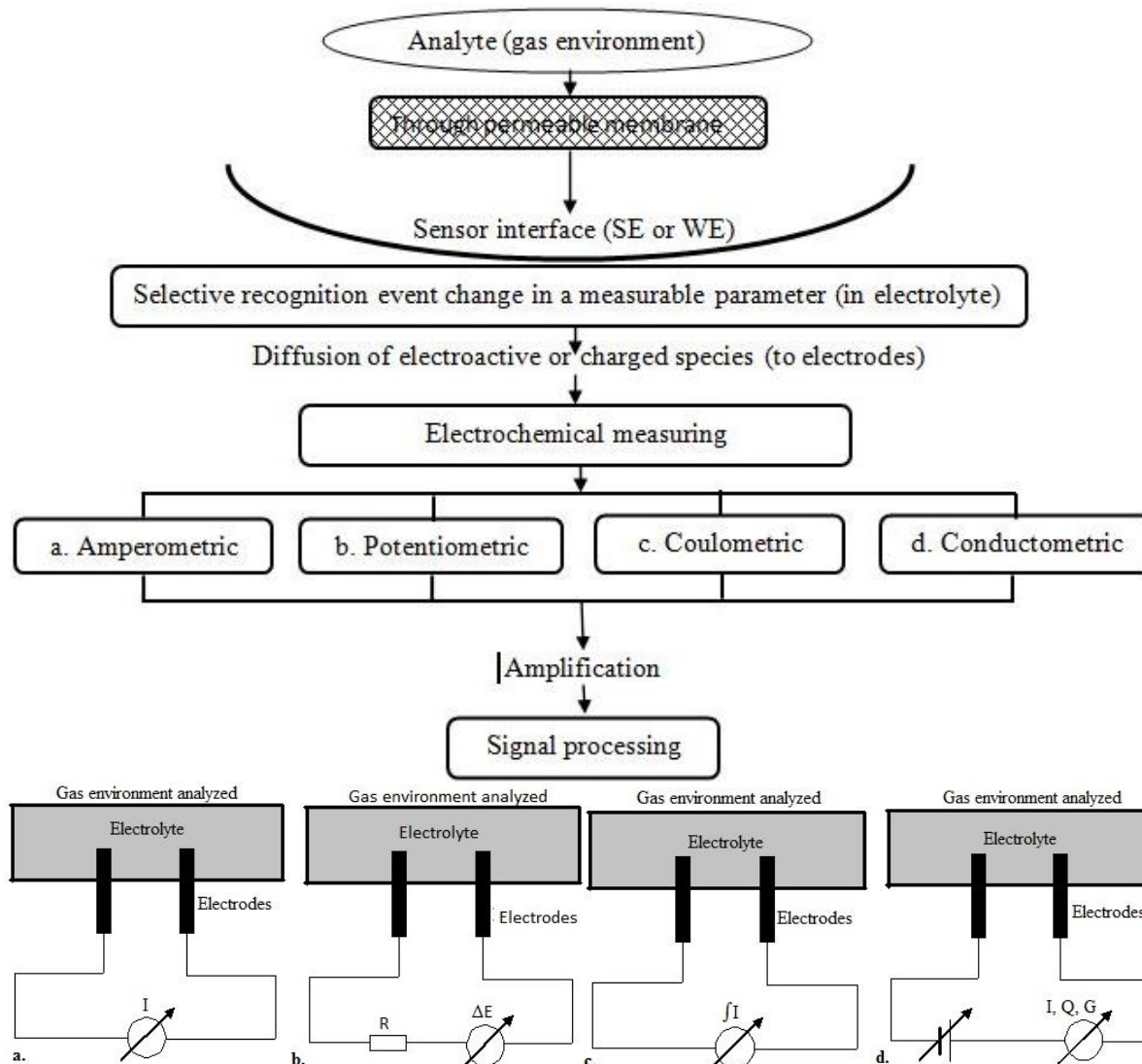


Figure 3. Schematic of working of a typical electrochemical gas sensor. Various detections involved (a) Amperometric detection (I = current) (b) Potentiometric detection (ΔE = voltage/potential difference) (c) Coulometric detection ($\int I$ is the charge in coulometric detectors obtained by integrating the current passing with respect to the time of electrochemical reaction) (d) Conductometric detection (Q = charge, I = current, G = conductivity) [31, 33].

On the basis of electric parameters to be measured, electrochemical gas sensors are classified into potentiometric, amperometric, coulometric and conductometric sensors. Amperometric sensor (Figure 3a) is based on the measurement of redox current (amperes) when electroactive species get reduced or oxidized, while keeping potential constant. In potentiometric sensor (Figure 3b), difference of electric potential (or voltage) is measured while maintaining a constant electric current (normally nearly zero) between the two electrodes. Coulometric sensors (Figure 3c) generate the analytical signal corresponding to the charge (coulombs) consumed involving the analyte. Conductometric sensors (Figure 3d) measures the change in resistance or the conductivity of electrolyte, while a constant alternating-current (AC) potential is maintained between the two electrodes. Amperometric and potentiometric sensors are mostly used for the detection of gases, while coulometric and conductometric sensors are rarely applied to gas sensing [31, 32].

The work carried on the detection of toxic gases by electrochemical sensors till now is huge and it is not possible to summarize sensing of every individual toxic gas in a single review. However, in this review effort has been made to cover some of the advance concepts incorporated in the development of electrochemical gas sensors due to the strength of nanotechnology that improved basic quality assurance parameters of electrochemical sensors for monitoring of NH_3 , H_2S and NO_x toxic gases. Forthcoming part is divided into various sections, each describing the detection of individual gas.

2. DETECTION OF NH_3 GAS

Ammonia is a natural gas and its contents in the atmosphere are increasing because of human activities. European commission for the environment and quality of life estimated the value of NH_3 emission throughout the world to be 20-30 Tg (1 Tg = 10^{12}g) [34]. Other results, summarized by Warneck [35] showed value of NH_3 emission in the range of 20-80Tg. Higher concentrations (1000 ppm or more) of NH_3 may cause pulmonary oedema, accumulation of fluid in the lungs and even death. Due to its acute toxicity; development of highly selective, stable, reliable and cost effective sensor is strongly required.

So far, several methods have been employed to obtain a highly sensitive NH_3 sensor. For example, chemical stability and excellent conductivity of SnO_2 based sensors makes them promising candidates for NH_3 sensing. These sensors have high response and recovery time. However, the requirement of high temperature for optimal function as well as issues with sensitivity and selectivity are certain drawbacks associated with SnO_2 based devices. To overcome these problems, new sensors based on doping of SnO_2 materials (with metals and inorganic materials) have been designed which improved sensing characteristics of these sensors. For example, Li et al. [36] synthesized nanocomposite of SnO_2 /polypyrrole by vapor phase polymerization of pyrrole with camphor sulfonic acid (CSA), poly (4-styrenesulfonic acid) (PSSA), hydrochloric acid (HCl) and *p*-toluenesulfonic (TSA) acids. The comparison between pure SnO_2 nanosheet and SnO_2 /PPy based sensors were made. It was observed that pure SnO_2 nanosheet showed not only poor response towards NH_3 gas but also negligible conductivity at room temperature, while as the SnO_2 /PPy based sensors showed enhanced

sensitivity towards NH_3 gas. The response of dopants for 1-10.7 ppm NH_3 decreased in this order $\text{PSSA} > \text{HCl} > \text{TSA} > \text{CSA}$. The effect of polymerization time of pyrrole was studied on sensing properties of these nanocomposites and it was revealed that when the polymerization time was increased from 0.5 to 1 hour, it resulted in the increase of the response magnitude (S) of the sensor. The detection limit of the sensor was investigated to be 257 ppb and sensitivity was in the range of 6.2% for 1-10.7 ppm NH_3 . The enhanced sensing characteristic was attributed to the fact that SnO_2 nanosheets and PPy coatings form a p/n junction at their interface. These nanostructures have high surface to volume ratio as well as substrate and sensing material has good ohmic contact. These factors were considered to be responsible for enhanced performance of the device.

Xu et al. [37] studied the properties of one dimensional (1D) alkaline earth metal composite SnO_2 nanofibers (5-7nm) for NH_3 sensing. These alkaline earth metals have excellent ability to control the growth of grain and resulted in enhanced chemisorptions of oxygen. These attributes make them ideal candidates for gas sensing applications. Comparison of Sr/ SnO_2 sensor with pristine SnO_2 sensor showed that the former has higher sensitivity, lower detection limit of 10ppm and response time of 6 s towards 2000 ppm, 12.67 s for 100 ppm and ~ 16 s towards 10 ppm which was much better than the pristine SnO_2 sensing platform. The fast response of Sr/ SnO_2 sensor was attributed to enhanced adsorption of oxygen by their tubular structures with enhanced electrical conductivity. It was also found that carrier density of Sr/ SnO_2 was 3 folds higher than pristine SnO_2 indicated by Mott-Schottky plots (M-S) and electrochemical impedance spectroscopy (EIS) measurements.

Another report shows the exploitation of cobalt oxide (Co_3O_4) for sensing applications where Deng et al. [38] reported the hierarchical structure of Co_3O_4 nanorods synthesized by the hydrothermal method. It was demonstrated that hierarchical Co_3O_4 nanorods showed instant response (2 s) and recovery time (10 s) for NH_3 gas in comparison to pure Co_3O_4 nanorods with slow response (100 s) and recovery time (50 s). Such an enhanced response was attributed to the high surface area of hierarchical Co_3O_4 nanorods while at the same time porous nanostructure allowed gas molecules to diffuse easily, resulting in increased response.

Wu et al. [39] studied the properties of 3D hierarchical porous Co_3O_4 materials (HPCo) for NH_3 gas sensing. These 3D materials with interconnecting mesopores and micropores showed enhanced sensitivity (146% to 100 ppm NH_3), response time (2s for 100ppm) and detection limit (0.5 ppm). Such an enhanced performance was due to the presence of defects which improved the adsorption of the gas molecules.

Similarly, Lin et al. [40] fabricated a sensor based on Co_3O_4 /polyethyleneimine-carbon nanotubes nanocomposites (CoPCNTs) where nanoparticles of Co_3O_4 (5-10nm) were loaded on PCNTs (grown at 160°C). These nanocomposites showed higher response time (4.3 s) for NH_3 and CO (4 s) gases at room temperature. The detection limit for CO and NH_3 was found to be 5ppm and 1ppm respectively. Such enhanced sensing properties were again attributed to the fact that due to low Schottky barrier, work function between Co_3O_4 NPs (4.5eV) and CNTs (4.7-4.9eV) was found to be very close which helped in the flow of electrons effectively. These sensors exhibited good response and recovery time when exposed to three cycles of gases, indicating their high stability and potential for industrial applications.

The mixed potential type sensors require solid electrolytes with two electrodes which play an important role in sensing NH_3 gas. These solid electrolytes should have the ability to transfer oxygen ions between reference electrodes to sensing electrode. A recent attempt showed the use of apatite-type lanthanum silicates ($\text{La}_{10}\text{Si}_5\text{MgO}_{26}$ (LSMO)) as solid electrolyte for sensing NH_3 gas [41]. This sensor showed enhanced response time (11s) and recovery time (13s) at 200ppm-300ppm of NH_3 . Similarly, Meng et al. [42] fabricated mixed potential sensor by introducing $\text{La}_{10}\text{Si}_{5.5}\text{Al}_{0.5}\text{O}_{27}$ as a solid electrolyte and $\text{TiO}_2@\text{WO}_3$ as a sensing electrode where core shell composite of $\text{TiO}_2@\text{WO}_3$ was prepared by hydrothermal method. In this case sensor response for NH_3 at 400~550 °C was measured and the response (74.8 mV/decade) measured was higher in comparison to sensors based on pure TiO_2 or WO_3 . Sensitivities at 400, 450, 500 and 550 °C were found to be 52.8, 69.7, 61.9 and 37.7 mV/decade, respectively. This sensor showed enhanced selectivity towards NH_3 gas in the presence of NO_2 . Lian et al. [43] reported that a tubular NASICON (sodium super ionic conductor) based sensor with a porous Cr_2O_3 electrode doped with 10 % CNT showed excellent sensing performance towards 50-500ppm NH_3 in air at 200-250 °C.

Different novel methodologies involving the use of catalytic layers on sensing electrodes have resulted as one of the most effective technique for the improvement of NH_3 gas sensing characteristics. For example, a report shows that by lamination of a catalyst layer such as $\text{V}_2\text{O}_5\text{--WO}_3\text{--TiO}_2$ (VWT) or iron-containing zeolites (Fe-ZSM5) onto Au-SE, sensitivity of the sensor can be increased from -20 to -120 mV towards 470ppm NH_3 [44]. It has been observed that by using VWT, electrochemical activity of SE increased against NH_3 since it is believed to produce activated NH_3 species. In another study, the same group of scientists described non equilibrium behavior of the sensor device in light of mixed potential theory and analyzed the potential of $\text{Au} \mid \text{YSZ}$ (Yttria-stabilized zirconia) and $\text{Au-VWT} \mid \text{YSZ}$ half cells [45]. It was observed that the electrochemical reaction with NH_3 and NO occurs at the three-phase boundary (TPB). The shift of electrode potential due to NH_3 proves that when NH_3 reaches at TPB, it promotes electrode reaction itself and the products formed as a result of oxidation of NH_3 are not responsible for sensor effect. Moreover, the same group [46] investigated through electrochemical half cell measurements that in the case of electrode covered with selective catalytic reduction (SCR) catalyst, potential change was more pronounced. In a similar study Kamin el al. [47] fabricated a non-Nernstian electrochemical cell $\text{Au} \mid \text{YSZ} \mid \text{Au}, \text{V}_2\text{O}_5\text{--WO}_3\text{--TiO}_2$ (Figure 7a and 7b) for NH_3 sensing. In one case (Figure 4a), both electrodes are present on the same side of YSZ based sensor while in the other case for half cell model (Figure 4b), electrodes are at the top and bottom of YSZ substrate where Au electrode is deposited. Influence of V_2O_5 contents on the VWT catalyst layer towards NH_3 sensing properties was explored and it was observed that the catalytic activity increased due to increase in the contents of V_2O_5 resulting in improved adsorption capability. Influence of V_2O_5 contents on NH_3 sensing signals was also observed. For VWT 1.7, sensitivity of 45 mV per decade was obtained and for 3% V_2O_5 sensitivity increased up to 70 mV per decade NH_3 . However, for VWT 0, it decreased to 14 mV per decade (Figure 5).

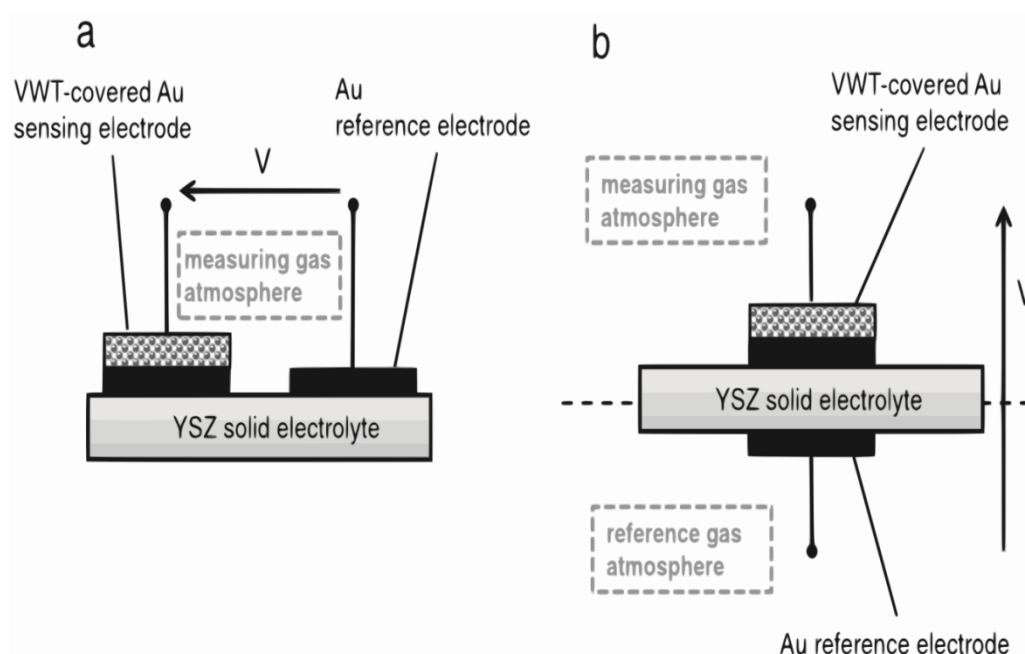


Figure 4. Schematic representation of the design of sensor structure (a) and of the half-cell model (b). This image was published in [47]. Copyright Elsevier (2013)

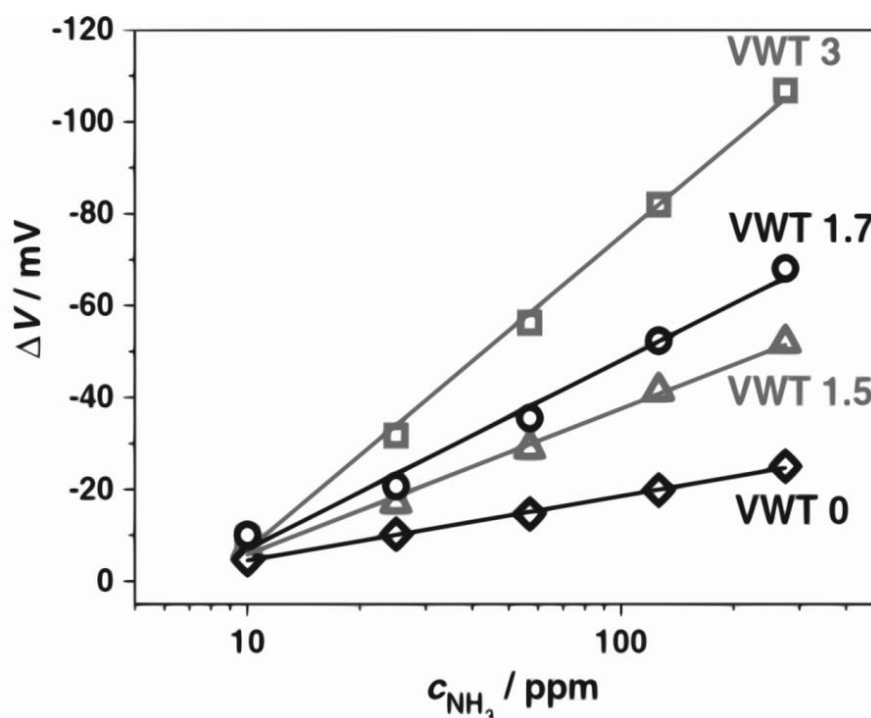


Figure 5. Semi-logarithmic NH_3 characteristic curves of "VWT, Au | YSZ | Au" sensor with changing V_2O_5 -contents of the layer of catalyst at 550 °C when both electrodes are exposed to measured gas: This image was published in [47]. Copyright Elsevier (2013)

In lab experiments, sensitivity of NH_3 gas is commonly evaluated by comparing sensitivities of SE towards various gases. However, in a real environment, NH_3 isn't present as a single gas but as a multi component mixtures e.g., Lee et al. [48] observed that sensitivity of YSZ based sensor using

In_2O_3 -SE decreased to 50 % from its original value when 150ppm of NO_2 was incorporated in a gas containing NH_3 . In order to avoid this problem, an oxide reference electrode of LaCoO_3 -RE was incorporated instead of Pt-RE. This reduced interference of NO_2 gas from 50 to 10 % and enhanced sensitivity towards ammonia gas. In another study, Li et al. [49] prepared $\text{Mg}_2\text{Cu}_x\text{Fe}_{1-x}\text{O}_{3.5+x}$ mixed metal oxides by co-precipitation method and used it to fabricate NH_3 sensor by screen printing $\text{Mg}_2\text{Cu}_x\text{Fe}_{1-x}\text{O}_{3.5+x}$ electrode on the surface of electrolyte. The catalyst was found to be effective for the oxidation of NH_3 gas where $\text{Mg}_2\text{Cu}_x\text{Fe}_{1-x}\text{O}_{3.5+x}$ electrode exhibited better sensitivity (226.6mV/decade) for NH_3 at 350 °C. Li et al. [50], also studied the effect of sintering temperature on $\text{Mg}_2\text{Cu}_{0.25}\text{Fe}_{1.75}\text{O}_{3.75}$ mixed metal oxides electrode for YSZ based potentiometric sensor. They separately sintered electrodes at 1000 °C, 1100 °C, 1200 °C, and 1300 °C and found that the electrode sintered at 1200 °C not only showed sensitivity in the range of 72 mV/decade NH_3 but also enhanced response (about 110 mV for 400 ppm NH_3) and recovery time in the range of 8-14s (Figure 6a and 6b). This is because of the reason that when $\text{Mg}_2\text{Cu}_{0.25}\text{Fe}_{1.75}\text{O}_{3.75}$ electrodes were sintered at 1200 °C, they exhibited three dimensional network structures where bigger grain size resulted into enhanced performance.

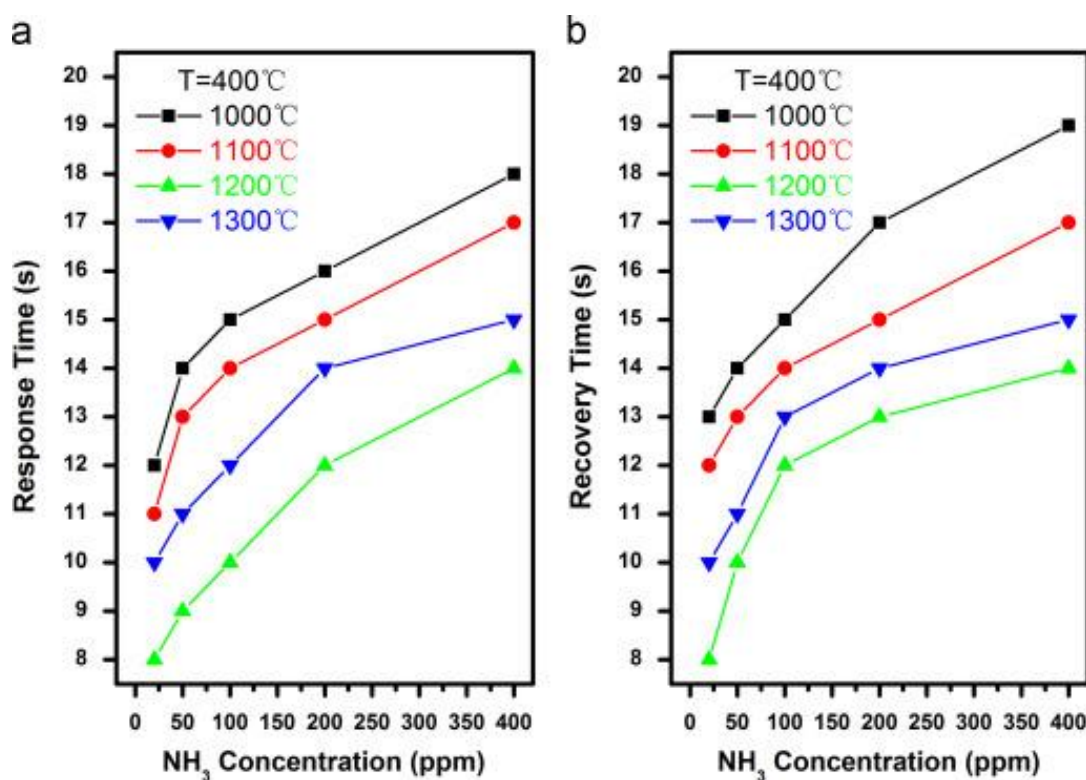


Figure 6. (a) Representing the response time and (b) the recovery time of NH_3 sensors with different sintered $\text{Mg}_2\text{Cu}_{0.25}\text{Fe}_{1.75}\text{O}_{3.75}$ electrodes to various NH_3 concentration at 400 °C. This image was published in [50]. Copyright Elsevier (2016)

Effect of sintering temperature on the sensing electrode for the detection of NH_3 gas was studied by Liu et al. [51]. This SE consists of $\text{Ni}_3\text{V}_2\text{O}_8$ as a new material in mixed potential YSZ based gas sensor. The $\text{Ni}_3\text{V}_2\text{O}_8$ calcined at 1000 °C showed higher sensitivity (−96 mV/decade) at 650 °C and the response to 100ppm NH_3 was found to be −62mV. A recent report shows the

development of planar type potentiometric sensor for the detection of odorants such as NH_3 , trimethyl amine, methyl mercaptan and H_2S [52]. The electrode potential of the planar type sensor ($\text{Au/YSZ}| \text{YSZ}| (\text{Pt/YSZ})$) responds to H_2S , trimethyl-amine, methyl mercaptan and NH_3 at sub-ppm level. The order of sensitivity was found to be methyl mercaptan $> \text{H}_2\text{S} > \text{NH}_3 >$ trimethylamine at 450°C [52]. Since the evaporation of electrolyte is often associated with the limited stability and short lifetime, aqueous electrolyte was replaced with ionic liquid (IL). Ionic liquids are considered as ideal electrolytes since they are non volatile and have high ionic conductivities. A recent report shows an electrochemical sensor for NH_3 detection consisting of a thin film of ionic liquid as an electrolyte and the planar micro-fabricated sensor which can detect ammonia as low as 1ppm in ambient conditions [53].

Screen printed electrodes (SPEs) are also considered as effective sensing surfaces due to their low cost and commercial accessibility. Many reports have been published recently using SPEs surface and room temperature ionic liquids (RTIL) as an electrolyte for the detection of toxic gases. For example, Murugappan et al. [54] reported that PtSPEs in combination with non-volatile RTILs are cost effective alternative for sensing of NH_3 compared to other amperometric materials. He studied voltammetry of NH_3 oxidation at room temperature using ionic liquid ($[\text{C}_2\text{mim}][\text{NTf}_2]$) on carbon, platinum and gold screen printed electrodes. It has been observed that clear and well defined oxidation peaks were obtained only on platinum and gold. However, due to possible interference of water impurities in the RTIL, the voltammetry on Au surface was found to be more complicated. A more simpler sensor design was investigated by Diao et al. [55] on using CoWO_4 -SE of YSZ based sensor system which showed faster response (less than 5s) and better sensitivity (-51 mV/decade) at elevated temperature.

Owing to high aspect ratio, unique physical and chemical properties, CNTs are also considered as ideal candidates for the fabrication of room temperature operate able sensors. Sensors based on Multi-walled carbon nanotubes (MWCNTs) show advantages over semiconductor based sensors considering simpler device architecture and high conductivity. Furthermore, the performance of MWCNTs based sensors can be enhanced by the addition of conducting polymers or other dopants. For example, Cui et al. [56] used Ag nanocrystals functionalized CNTs (Ag NC-MWCNTs) for the detection of NH_3 gas. Authors demonstrated the sensitivity of 9% when exposed to 1% NH_3 and the response was 7s. In this case, since the interaction of NH_3 gas with pristine CNT is weak, Ag NCs acted as a dominant adsorption region for ammonia thereby increasing the performance of the sensor. However, sensitivity of the developed sensor is still low and could be improved by further tuning the properties of CNTs.

Conducting polymers can also be considered as ideal candidates for room temperature working devices because of their low cost, fast response and reliability. A recent report investigated nanocomposites based PANI/MWCNTs for the detection of NH_3 gas. These sensors showed response to NH_3 in the concentration range of 2-10ppm [57]. In a similar study, nanocomposite of polypyrrole and carboxylated MWCNTs was investigated as an electrode material and was found to increase the ammonia sensitivity [58]. Abdullah et al. [57] reported a sensor based on polyaniline multi-walled carbon nanotubes (PANI/MWCNTS). These conducting polymers are cheap and showed fast response and higher sensitivity. The response time for PANI/MWCNTs based sensor was found to be 6s

(recovery time 35s), while in the case of pristine MWCNTs, it was much slower (965s, recovery time 24 minutes). The detection limit was found to be 2 ppm for NH_3 gas. Such an enhanced response was because of the coating of PANI on MWCNTs, resulting in increasing adsorption of NH_3 gas. However, further work is required regarding sensitivity and recovery time of such sensing systems in order to exploit them for commercial applications.

Therefore, owing to high surface area and enhanced reactivity, nanomaterials are ideal candidates to be explored as electrode materials for sensing number of toxic gases including NH_3 and hence further work on such materials is of significant importance.

3. DETECTION OF H_2S GAS

Hydrogen sulfide (H_2S) is a highly toxic gas, naturally present in crude petroleum, hot springs and food stuffs and commonly known as sewer gas, swamp gas and manure gas. When inhaled in excessive amounts, it causes broad spectrum poison and affects most parts of the body including nervous system. One source of its production is industries and places such as natural gas drilling, waste water treatment and landfills. H_2S is rapidly absorbed by lungs and when inhaled at high concentrations it causes unconsciousness and even death. Many electrochemical sensors have been fabricated recently for the detection of H_2S gas and research is still going on for the development of even sensitive, robust and cheap sensing devices.

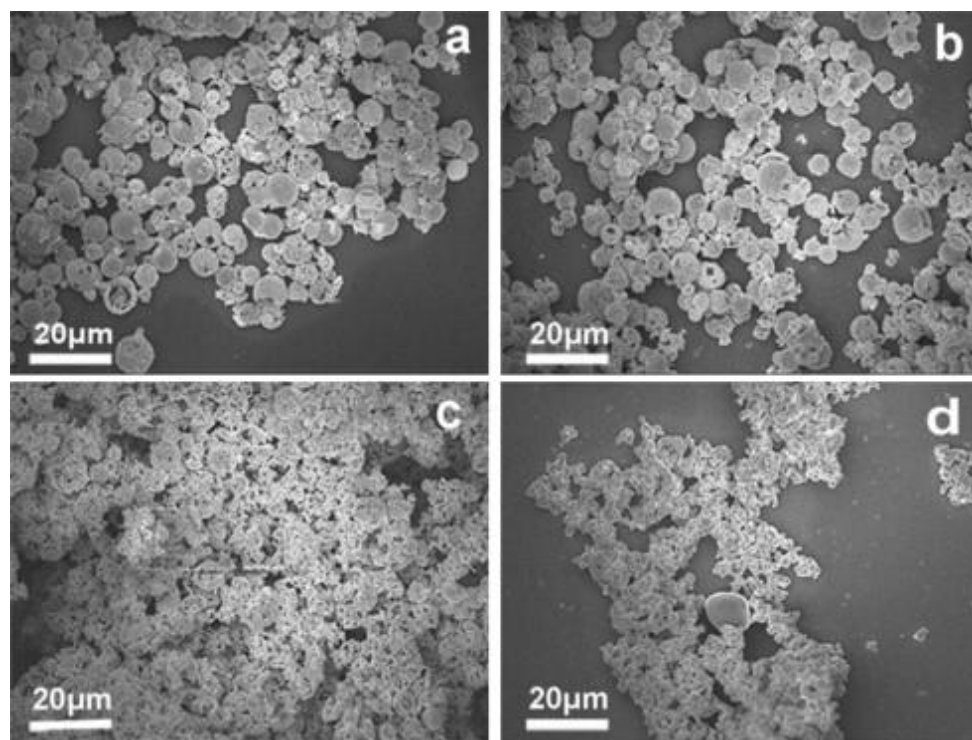


Figure 7. The SEM images of NiMn_2O_4 (2 s, 800–1100 °C). (a) NiMn_2O_4 (2 s, 800 °C), (b) NiMn_2O_4 (2 s, 900 °C), (c) NiMn_2O_4 (2 s, 1000 °C) and (d) NiMn_2O_4 (2 s, 1100 °C). This image was published in [59]. Copyright Elsevier (2013)

Guan et al. [59] prepared three oxides (NiMn_2O_4 , NiCr_2O_4 and NiFe_2O_4) by solvent evaporation method and used them as a sensing electrode of mixed potential type YSZ based H_2S sensor. Among them, hollow balls NiMn_2O_4 (5-8 μm diameter) exhibited higher sensitivity towards H_2S gas in the concentration range of 50ppb to 2ppm at 500 °C. The bigger holes in the hollow balls helped the low concentration gases to penetrate, resulting in the detection of gases with low concentrations. Scanning electron microscopy (SEM) images (Figure 7) show that NiMn_2O_4 (2s, 800°C) and NiMn_2O_4 (2s, 900°C) have better hollow structures which helped in the penetration of gases and increased sensitivity of a sensor. Moreover, by changing the dropping rate in sintering and solvent evaporation method, microstructures of the sensing material were modified resulting in enhanced sensitivity of electrode.

Figure 8 below shows the ΔV dependence on the logarithm of H_2S concentration for different sensors attached with varying NiMn_2O_4 concentrations observed at 500 °C. The highest ΔV and slope was obtained by NiMn_2O_4 with the detection limit of 50ppb.

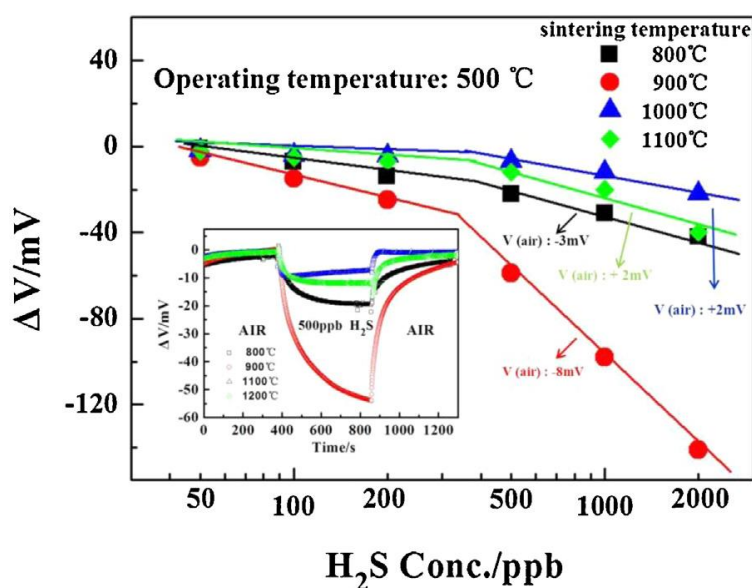


Figure 8. Dependence of the $\Delta V (V(\text{H}_2\text{S}) - V(\text{air}))$ on the logarithm of H_2S concentrations and the transients to 500 ppb H_2S for the sensors attached with NiMn_2O_4 (2 s, 800–1100 °C) at 500 °C. This image was published in [59]. Copyright Elsevier (2013)

High toxicity of H_2S gas in oil drilling rigs makes its detection a challenge for oil companies and hence all solid state potentiometric sensors are necessary to be developed. In an attempt, a new type of all solid state potentiometric sensor based on thick films of lithium lanthanum titanium oxide (LLTO) was developed which measured the concentration of sulfide ions in the drilling mud [60]. Such measurement was reported to be realized through the measurement of pH of the sample with the antimony/antimony oxide electrode.

Kim et al. [61] prepared one dimensional ZnO nanostructures through hydrothermal method and exploited such ZnO nanorod bundles for the detection of H_2S (Figure 9). A thick depletion region was formed when oxygen adsorbed on the bare ZnO nanorod surface (Scheme 9a). Upon exposure to

H₂S gas, a reaction with adsorbed oxygen occurred resulting in increased conductivity (Scheme 9b). A change in depletion region and band bending occurred due to change in oxygen concentration. When temperature is greater than 300°C, besides reaction with oxygen, H₂S decomposed and formed Zn-S bonds on the surface of ZnO resulting into the formation of shallow donor levels, responsible for drastic increase in conductivity (Scheme 9c) [61].

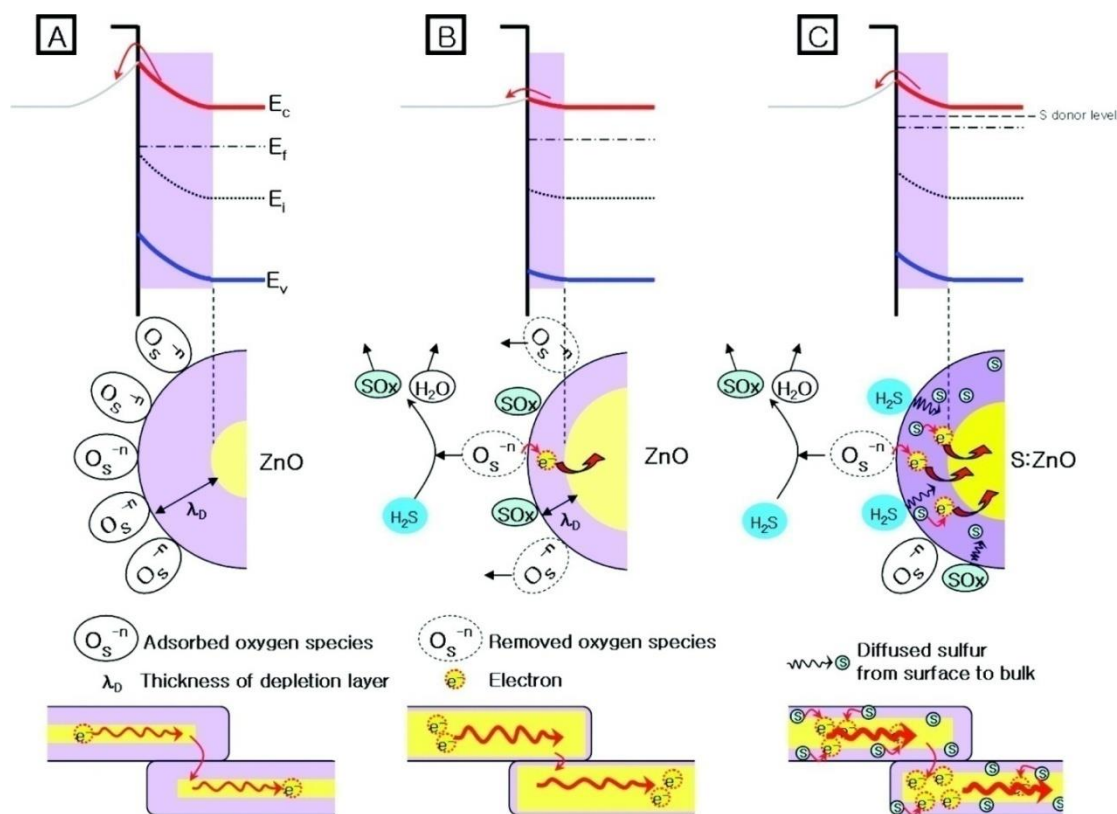


Figure 9. Band Diagrams and Schematic Image of Electric Properties of (a) Oxygen Ionosorption Surface before Sensing, (b) H₂S Gas Adsorption and Surface Reaction with Surface Oxygen and (c) Donor Level Formation of ZnO Nanorod Bundles with Sulfur Chemisorption at $T_s > 300^\circ\text{C}$. Reproduced with permission from [61]. Copyright American Chemical Society (2011)

Hosseini et al. [62] synthesized vertically aligned rods of ZnO through vapor phase transport (VPT) method and sensing parameters of grown nanostructures were measured for H₂S gas at room temperature and at 250 °C. It was found that sensing response increased with increase in the concentration of H₂S gas at room temperature. They could also measure the transient response curves for sensor towards H₂S (1 and 5ppm) at room temperature and at 250°C. A better response (e.g. $S = 296$ at 1 ppm and 581 at 5 ppm) and enhanced selectivity was observed at room temperature and at 250°C. Same group of scientists synthesized ZnO rods on bare Si substrate by VPT method [63] where modification was achieved by incorporating Au (6nm thick) which enhanced sensing performance of H₂S sensor (response was about 1270 at 6 ppm H₂S gas).

Hierarchical nanostructures also play significant role in improving sensitivity and response time for a particular sensor. For example, Yin et al. [64] synthesized hierarchical SnO₂-rGO nanostructures and used them in sensing of H₂S gas. This sensor showed enhanced sensitivity of up to

78 for 10ppm H₂S at 100 °C with the response time of 7 seconds. In order to get low detection limit, several nanorods were also employed in electrochemical sensors for monitoring toxic gases. For example, Lanh et al. [65] used seed mediated method for the growth of different Au nanorods which exhibited higher sensitivity and fast response towards H₂S gas at low concentration (2.5–10 ppm) in the temperature range of 300 °C to 400 °C.

In certain cases, sensing is required to be carried out at high temperatures where materials requirement is also different compared to measurements at room temperatures. In an attempt to fabricate such sensor, fabrication of solid electrochemical sensor using electrode of CoCr_{1.2}Mn_{0.8}O₄ was carried out. The fabricated sensor showed response of 178 mV for 10ppm H₂S gas at 250 °C with good sensitivity and selectivity [66]. Similarly, Baker et al. [67] has also fabricated porous silicon (PS) conductometric sensor for the detection of H₂S gas in the concentration range of 0.6 to 100ppm. They also investigated the response of PS interface towards H₂S gas detection when it was decorated with different metal oxides. It was observed that response of Au_xO decorated PS interface has better response than other metal oxides. However, on the basis of selectivity SnO_x decorated PS showed higher selectivity towards H₂S.

Due to high surface to volume ratio with excellent optical and electronic properties, Carbon nanotubes are ideal candidates to be employed in sensing H₂S. Asad et al. [68] demonstrated that Cu-SWCNTs-based sensors showed higher response towards various concentrations of H₂S gas ranging from 5ppm to 150ppm with the faster response and recovery time of 10s and 15 seconds. Further work on such systems is required, especially by exploiting vertically aligned CNTs for sensing of toxic gases. In another study, MalekAlaie et al. [69] fabricated H₂S gas sensor by spin coating molybdenum trioxide (MoO₃) nanoparticles decorated rGO on Al₂O₃ substrate between platinum electrodes. These MoO₃ nanoparticles (*n*-type) acted as a promoter and their addition on rGO (*p*-type) by impregnation method resulted in the formation of two depletion regions at the interface. When this system was employed for the sensing of H₂S gas, it resulted in the change of potential barrier between MoO₃ nanoparticles and rGO interface which caused the change of electrical resistance. Effect of change of various concentrations of MoO₃ nanoparticles on the performance of sensor has also been studied where 3 wt% MoO₃ showed the best response towards H₂S gas with average resistance in the range of 21±5 kΩ at a temperature of 160 °C. This sensor showed fast response of about 60 s after 50 ppm exposure of H₂S gas with the recovery time of 120s. This device was found to be highly selective towards H₂S gas when compared with NO, CO and ethanol.

One dimensional nanostructures have also attracted considerable attention of scientists due to superior spatial resolution and higher response and recovery time owing to a high surface and volume ratio. In order to investigate the role of 1D nanostructures towards sensing performance of H₂S gas, Kim et al. [70] reported a comparison between bare CuO nanorods based sensor and Pd functionalized CuO nanorods. In this case, when 1D CuO nanostructures were exposed to H₂S gas, formation of CuS layer at the surface of CuO nanorods was observed. When the supply of H₂S gas was stopped, the oxidation of CuS layer occurred, converting it back to CuO. The sensing behavior of the nanorods in this case was due to the oxidation of CuS layer. In the presence of Pd, rate of adsorption of H₂S gas molecules at the surface of sensing layer increased where chemisorbed oxygen species were formed more rapidly upon dissociation of H₂S molecules. Thus, higher response (31,243%) was observed in

the case of Pd functionalized Cu nanorods based sensor. In order to further exploit *p*-type CuO semiconductor properties, Ayesh et al. [71] reported the H₂S gas sensor with embedded CuO nanoparticles within poly vinyl- alcohol (PVA) membrane and glycerol ionic liquid (IL). These CuO nanoparticles have high affinity towards H₂S gas due to high surface to volume ratio and efficient adsorption of ions. When CuO nanoparticles were embedded in solution of PVA and 5% IL, these sensors exhibited fast response of 20.4 ± 12.8 s.

Nanomaterials are considered to be the promising candidates in the field of electrochemical sensing owing to their unique physical and chemical properties. For H₂S sensing, Gutes et al. [72] first used nanoparticles decorated with graphene because of its high conductivity. They decorated metal nanoparticles of platinum, gold and palladium on the CVD grown graphene. They observed that Pd and Au had higher nanoparticle density than platinum. It was revealed that gold nanoparticles doped graphene showed sensitivity towards H₂S gas but recovery time was too slow. This was due to formation of a strong S-Au bond. For detection of H₂S gas, Zhou et al. [73] synthesized stable nanocrystals of Cu₂O (3nm) and grew them on the functionalized sheet of graphene. Functionalized sheet of graphene played an important role in the prevention of unfavorable aggregation, lowering nucleation process and controlling the nucleation sites. Instead of using any capping agent such as surfactants, these functionalized sheets acted as molecular template, resulting in enhanced sensitivity, even when 5ppb H₂S gas was exposed to the sensor at room temperature. The enhanced sensitivity was attributed to the availability of more active sites since Cu₂O nanoparticles were not capped with any surfactant. Towards exploiting graphene based materials for sensing toxic gases, Alaie et al. [74] has discussed properties of graphene oxide for ultra sensitive detection of H₂S gas. A change in electronic structure of GO has been observed when gases were physisorbed or chemisorbed on its surface, hence acting as electron donor or acceptor materials. They functionalized GO with Dodecylamine (DDA) and ethylenediamine (EDA) owing to the fact that they have a high affinity for H₂S gas. In this case, response time was observed to be 60s when exposed to the H₂S gas while this sensor also showed higher sensitivity towards H₂S gas in the presence of other interfering gases such as CO, NO and ethanol. Unlike pristine graphene oxide (GO) based sensor, sensor with dodecylamine-GO and ethylenediamine-GO chemiresistors showed significant response towards H₂S gas (50ppm at room temperature).

Cuong et al. [75] demonstrated a simple solution phase method for the fabrication of ZnO-graphene gas sensor. This sensor was able to detect H₂S gas in the range of 2 ppm in the presence of oxygen at room temperature. The presence of oxygen played significant role in enhanced performance of the sensor which was attributed to the stronger interactions of H₂S gas molecules with the adsorbed oxygen at the surface of ZnO nanorods. Authors did not investigate on the cross-sensitivity which was considered to be the major issue in the present study. Ramgir et al. [76] compared the performance of *p*-type ZnO nanoparticles and *n*-types ZnO nanowires by using a simple chemical process. Both materials showed enhanced response and recovery time. Although this sensor was selective towards H₂S gas but also showed partial selectivity towards chlorine. Similarly, Zhao et al. [77] compared the performance of CuO doped ZnO nanofibers with pure ZnO nanofibers towards sensing H₂S gas where CuO doped ZnO nanofibers showed enhanced sensitivity towards H₂S gas compared to pure ZnO nanofibers. However, no significant change in response and recovery time was observed between

devices made up of two materials. The sensing mechanism for ZnO based sensors was attributed to the adsorption and desorption of target gas at the surface of material.

4. DETECTION OF NO_x GASES

Oxides of nitrogen (NO and NO₂ collectively known as NO_x) are responsible for several adverse effects to our atmosphere. These effects mainly include addition to global warming as these oxides readily react with ozone leading to its depletion. Inhalation of these oxides causes respiratory problems [78, 79]. The demand for monitoring of these gases is increasing to control environmental pollution and the electrochemical sensors have proven to be one of most reliable devices for the detection of NO_x gases. In case, monitoring of NO_x gases in vehicle exhausts is required, the sensor has to be operating at the temperature of 550-900 °C.

Different methodologies to enhance NO₂ sensitivity including designing of unique sensor geometry with different ratios of oxides have been reported [80]. Different ratios of W/Cr oxide were studied and it was investigated that oxide with 3:2 W/Cr showed best response value of 51.6 mV for 100ppm NO₂ with a response time less than 20 seconds. Moreover, best performance was obtained by a device which was sintered at 1000 °C. In another approach, Prakash et al. [81] investigated that the electrochemical activity of CuNP-SWCNT-PPy-Pt electrode was found to be four times higher than CuNP-PPy-Pt electrode. Sensitivity of electrode was $0.22 \pm 0.002 \mu\text{A } \mu\text{M}^{-1} \text{ cm}^{-2}$ with 0.7 μM detection limit.

Striker et al; [82] compared response of high surface area (HSA) nanocomposite with that of low surface area (LSA) Au sensing electrode and found that LSA Au-YSZ electrode has higher sensitivity for all gases, more than twice the selectivity of HSA Au electrode towards NO₂ and CO gases. Elucidation of the Au role in enhancing NO_x sensitivity has been explored by using YSZ based mixed potentiometric sensor. Elvan Romanytsia et al. [83] compared the sensitivity of YSZ based planar sensor (Au + 10 wt% YSZ)/YSZ/Pt with a reference sensor Au/YSZ/Pt towards NO₂. It was observed that (Au + 10 wt% YSZ)/YSZ/Pt has a shorter response time and better sensitivity (20–100 ppm for NO₂ at 450 to 550°C) than Au/YSZ/Pt sensor. The incorporation of YSZ into Au electrode enhances mixed ionic and electronic conductivity as a result triple phase boundary (TPB) volume gets delocalized and sensitivity gets better.

Another alternative method to minimize the cross selectivity to other gases is proposed by Yan et al. [84] where they fabricated ZnO nanostructures/PS (porous silicon) gas sensor for the detection of NO₂ gas. They first etched P-type silicon wafer electrochemically in a solution for eight minutes with a constant current density of 100 mA/cm². After separating cell into two half cells by silicon wafer, Pt electrodes were immersed in each half cell in an electrolyte (Figure 10). It was observed that proposed sensor showed enhanced gas sensing properties of PS with the addition of nanosheets of ZnO. Such sensor was found to show limit of detection of 100ppb; response time from 200s to 90s and recovery time of 180s to 120s respectively.

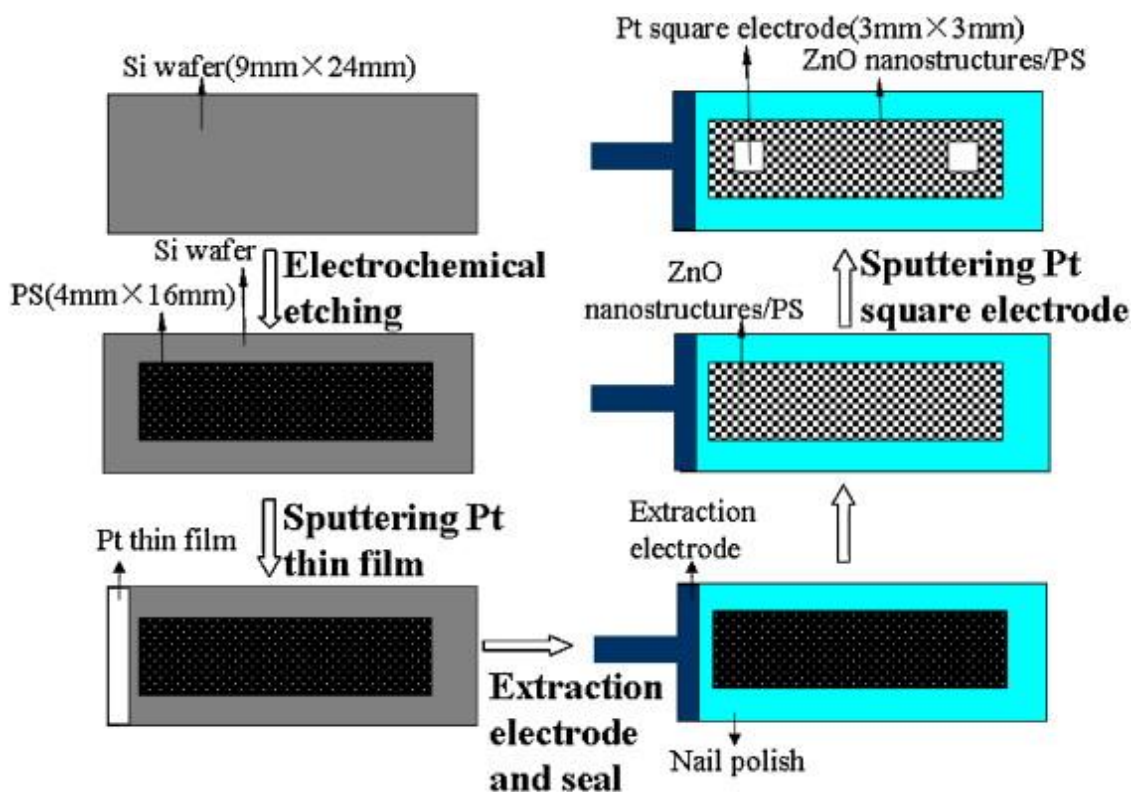


Figure 10. The schematic diagram of the process flow for the preparation of ZnO nanostructures/PS sensor. This image was published in [84]. Copyright Elsevier (2013)

Apart from being able to detect NO_x selectively, a high-performance solid electrolyte sensor is also defined by its ability to provide a rapid sensing signal. One example of such sensor was reported by Paściak et al. [85] who studied the performance of solid electrolyte of super-ionic conductor $\text{Na}_{3.4}\text{Zr}_2\text{P}_{0.6}\text{Si}_{2.4}\text{O}_{12}$ (NASICON) in potentiometric NO_x sensor. The proposed sensor showed sensing properties in the range of 10-1000ppm. Gao et al. [86] fabricated YSZ based sensor by screen printed technology using two metallic electrodes of Au and Pt. The proposed sensor showed enhance selectivity towards NO_x sensing using a catalytic filter (1.7 wt% Pt dispersed on alumina) directly on sensing electrode. For the detection of exhaust gases, Gándara et al. [87] proposed a YSZ based potentiometric sensor for the detection of NO gas and observed that addition of 20 micrometer layer of WO_3 and porous YSZ on sensing electrode enhanced the sensitivity of sensor and also improved response time.

Shahid et al. [88] reported the synthesis and fabrication of (rGO- Co_3O_4 @Pt) nanocomposite on glassy carbon electrode and studied its sensitivity towards NO gas. They found improved sensitivity while limit of detection obtained was $1.73 \mu\text{M}$ with a signal-to-noise (S/N) ratio of ~ 3 using the amperometric $i-t$ curve technique. A recent report shows the MEMS-based amperometric nitric oxide (NO) gas sensor for the purpose of asthma monitoring [89] where microporous high surface electrode coated with Nafion was used and showed sensitivity of 0.045nA/ppb . Another similar kind of report used an array of 15 sensors connected in series to monitor NO_x gases at 550°C [90] and reported the

sensitivity at the 50ppb. Very recent studies show the use of nano-structured perovskite-type oxide $\text{Gd}_{0.2}\text{Sr}_{0.8}\text{FeO}_{3-\delta}$ (GSF) as sensing-electrode (SE) and YSZ as solid electrolyte to detect NO_x gas in the concentration range of 25 to 500ppm at 500-800°C [91]. Due to enhanced surface area of triple phase boundary (TPB), Chen et al. [92] described YSZ based potentiometric sensor with La_2CuO_4 sensing electrode for the detection of NO and NO_2 gases. By addition of YSZ in different concentrations into La_2CuO_4 enhanced superficial area of TPB. It has been observed that sensor fabricated with 5 vol % YSZ shows higher sensitivity towards NO at 400 °C.

Zheng et al. [93] recently demonstrated an improved amperometric Pt–Nafion sensor which showed higher sensitivity ($880 \pm 60 \text{ pA ppb}^{-1}$), lower detection limit ($4.3 \pm 1.1 \text{ ppb}$), active surface mass area ($34 \pm 9 \text{ cm}^2$) and a faster response time ($<5\text{s}$) towards NO_x . The general design of the sensor was such that it has reference electrode of single junction Ag/AgCl and a bare Pt counter electrode along with 0.5 M H_2SO_4 internal electrolyte (Figure 11). They deposited Pt electrode on a Nafion 117 membrane (an ion exchange membrane) by infusing the film with ions, which were then subjected to NaBH_4 in order to precipitate noble metals. Moreover, results for sensitivity of amperometric Pt–Nafion $\text{Pt}(\text{NH}_3)_4^{2+}$ sensor and chemiluminescence was correlated for monitoring of NO_x which released from Carbosil2080A polymer films doped with *S*-nitroso-*N*-acetylpenicillamine.

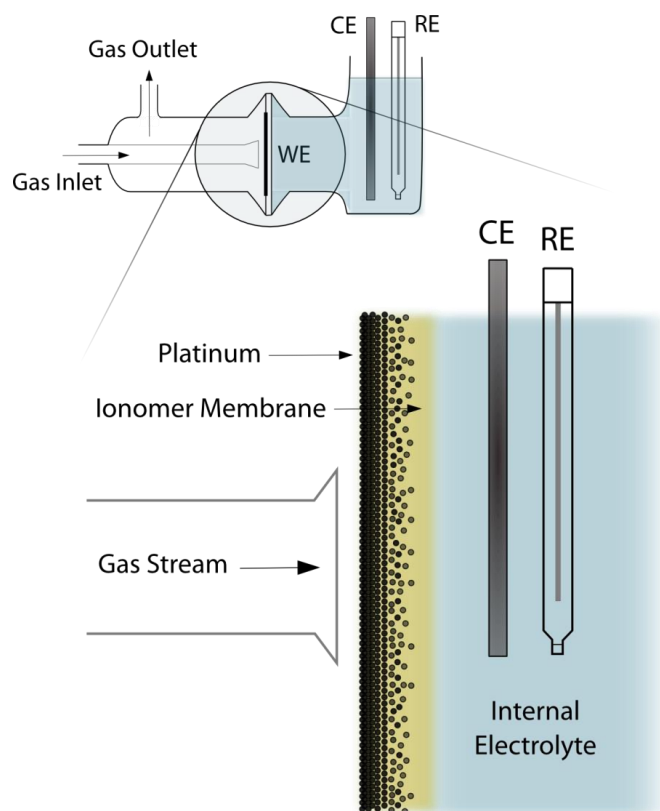


Figure 11. Schematic illustration of SPE-based NO Sensor. WE = Pt–Nafion; CE = bare Pt; RE = single-junction Ag/AgCl in saturated KCl; internal electrolyte = 0.5 M H_2SO_4 . This image was published in [93]. Copyright Elsevier (2015)

Berisha et al. [94] have optimized the working parameters of a carbon heterogeneous electrodes sensor modified with chromium (III) oxide for the detection of NO. Compared to unmodified

electrode, the electrode modified with chromium (III) improved the performance of the sensor. They have also determined the influence of interfering gases and observed no effect to nitrate but found that nitrite interferes if present in higher concentrations than the analyte. Wang et al. [95] reported an apatite-type $\text{La}_{10}\text{Si}_5\text{AlO}_{26.5}$ as an electrolyte with Ag-modified nano-structured CuO sensing electrode for the amperometric NO_2 sensing. The proposed sensor showed not only good response to NO_2 but response current was also found to be linear to the concentration of NO_2 in the range of 0–500 ppm at 550–700 °C. By the addition of Ag into CuO sensing electrode sensitivity was found to enhance. Among all variations to fabricate sensors for the detection of NO_x , sensing system based on electrodes comprising nanomaterials showed potential for further investigations and require to be explored further.

5. CONCLUSIONS AND FUTURE PERSPECTIVES

Recently, scientists have progressed significantly in the area of sensing by exploiting the fundamental properties of nanomaterials. There have been many exciting developments in the field of electrochemical gas sensors for the detection of NH_3 , H_2S and NO_x toxic gases. The use of nanomaterials in electrochemical gas sensors have resulted in fabrication of more powerful tools for effective monitoring and detection of toxic gases even at sub-ppm level. These nanomaterials based electrochemical sensors have many advantages including miniaturization, better selectivity, enhanced sensitivity, portability and improved response and recovery time. This could be attributed to the high surface to volume ratio of the nanomaterials and also because such materials adsorb and desorb molecules frequently at their surfaces. With the passage of time, these gas sensor devices are becoming more flexible and sophisticated. The data presented mostly demonstrate that the single oxides such as ZnO, NiO, Cr_2O_3 for sensing electrode have been reported as potential candidates for gas sensing applications. In addition to metal oxides, various mixed metal oxide sensors [96, 97] as well as use of various additives such as noble metals and transition metal oxides [98] have shown potential in improving the sensing performance of electrochemical sensors.

However; despite many improvements and advantages, there are still several drawbacks associated with these sensors such as stability, reproducibility and limited use that needs to be addressed. To overcome such drawbacks, focus should be on the cost effective fabrication protocols, long-term stability and robustness of the sensing devices. Furthermore, electrochemical gas sensors are also facing challenges in the area of electrolyte. Many publications have focused on oxygen conducting electrolytes in mixed potential gas sensors [99]. However, these sensors have poor temporal stability and selectivity. Therefore, present focus is on proton conducting electrolytes due to their stability and better electron transporting property [100]. In order to develop electrochemical sensors for desired applications, materials properties of the electrode are required to be modified and optimized. For a selective, sensitive and long term stable sensors more comprehensive understanding about the correlations between material parameters regarding chemical composition and grain size is required. By using micro and nano electrodes, a rapid sensor response can be obtained. Integration of gas sensors in microelectronics and portable devices also faces challenge of power consumption and

generation of heat. Recently, Moon et al.[101] introduced self assembled nano columnar WO₃ thin films on glass substrate which produced response to NO_x by using less than 0.2 microwatt power. This exceptional effect of nano-columnar sensor was attributed to the synergistic effect of high surface to volume ratio of WO₃, self heating and the presence of narrow necks between the columns. Further work using similar kind of approaches is essentially required in order to deal with limitations of electrochemical sensing platform.

To sum up, area of electrochemical sensing of toxic gases is of significant importance indicated by the frequency of recently published works. However, in the area of stability and reproducibility, many challenges still exist and required to be addressed. Although, many improvements in sensitivity, selectivity and response time have already been achieved but more sophisticated systems, combining and integrating online sampling and separation steps, are crucial to fabricate more sensitive and selective sensing system. As most of these sensors are tested in laboratory conditions, they need to be studied in more details for operating in harsh environmental conditions. Regarding fabricating sensing system which is more robust, sensitive, cheap and selective, further exploitation of nanomaterials of various types and dimensions is of significant value.

ACKNOWLEDGEMENT

Z.H. gratefully acknowledges financial support from the Higher Education Commission (HEC) of Pakistan under NRPU project No. 20-3066/NRPU/R&D/HEC/13.

References

1. L. Rassaei, F. Marken, M. Sillanpää, M. Amiri, C. M. Cirtiu, and M. Sillanpää, *Trends. Anal. Chem. TRAC*, 30 (2011) 1704.
2. E. Llobet, *Sens. Actuator B-Chem.*, 179 (2013) 32.
3. J. W. Fergus, *Sens. Actuator B-Chem.*, 134 (2008) 1034-1041.
4. K. Wetchakun, T. Samerjai, N. Tamaekong, C. Liewhiran, C. Siri Wong, V. Kruefu, A. Wisitsoraat, A. Tuantranont, and S. Phanichphant, *Sens. Actuator B-Chem.*, 160 (2011) 580.
5. B. Timmer, W. Olthuis, and A. Van Den Berg, *Sens. Actuator B-Chem.*, 107 (2005) 666.
6. B. Spilker, J. Randhahn, H. Grabow, H. Beikirch, and P. Jeroschewski, *J. Electroanal. Chem.*, 612 (2008) 121.
7. N. Miura, Y. Yan, G. Lu, and N. Yamazoe, *Sens. Actuator B-Chem.*, 34 (1996) 367.
8. J. E. Ryer-Powder, *Plant/operations progress.*, 10 (1991) 228.
9. P. Teerapanich, M. T. Z. Myint, C. M. Joseph, G. L. Hornyak, and J. Dutta, *IEEE Trans. Nanotechnol.*, 12 (2013) 255.
10. D. M. Bolstad-Johnson, J. L. Burgess, C. D. Crutchfield, S. Storment, R. Gerkin, and J. R. Wilson, *Am. Ind. Hyg. Assoc. J.*, 61 (2000) 636.
11. S. K. Pandey, K.-H. Kim, and K.-T. Tang, *Trends. Anal. Chem. TRAC*, 32 (2012) 87.
12. L. P. Martin, A.-Q. Pham, and R. S. Glass, *Solid State Ionics*, 175 (2004) 527.
13. S. Barnes and L. T. Old, *Chem. Eng. Prog.*, 105 (2009) 51.
14. A. Chiorino, G. Ghiotti, F. Prinetto, M. Carotta, D. Gnani, and G. Martinelli, *Sens. Actuator B-Chem.*, 58 (1999) 338.
15. M. Suresh, N. J. Vasa, V. Agarwal, and J. Chandapillai, *Sens. Actuator B-Chem.*, 195 (2014) 44.
16. C. Di Natale, V. Ferrari, A. Ponzoni, G. Sberveglieri, and M. Ferrari, *Sensors and*

- Microsystems: Proceedings of the 17th National Conference, Brescia, Italy, 5-7 February 2013.*, 268 (2013) Springer Science & Business Media.
17. C. Li and G. Shi, *J. Photochem. Photobiol., C: Photochem. Rev.*, 19 (2014) 20.
 18. Q. Zhu and R. C. Aller, *Mar. Chem.*, 157 (2013) 49.
 19. R. Jackson, R. P. Oda, R. K. Bhandari, S. B. Mahon, M. Brenner, G. A. Rockwood, and B.A. Logue, *Anal. Chem.*, 86 (2014) 1845.
 20. K. Zakrzewska, *Thin solid films*, 391 (2001) 229.
 21. Z. Darmastuti, C. Bur, P. Möller, R. Rahlin, N. Lindqvist, M. Andersson, A. Schütze, A. Lloyd Spetz, *Sens. Actuator B-Chem.*, 194 (2014) 511.
 22. N. S. Lawrence, L. Jiang, T. G. Jones, and R. G. Compton, *Anal. Chem.*, 75 (2003) 2499.
 23. E. Jones, *Techniques and mechanism in gas sensing.*, (1987) 17.
 24. J. W. Fergus, *Sens. Actuator B-Chem.*, 123 (2007) 1169.
 25. X. Liu, S. Cheng, H. Liu, S. Hu, D. Zhang, and H. Ning, *Sensors*, 12 (2012) 9635.
 26. A. W. E. Hodgson, P. Jacquinet, L. R. Jordan, and P. C. Hauser, *Anal Chim Acta*, 393 (1999) 43.
 27. E. Bakker and M. Telting-Diaz, *Anal. Chem.*, 74 (2002) 2781.
 28. G. Alberti, F. Cherubini, and R. Palombari, *Sens. Actuator B-Chem.*, 37 (1996) 131.
 29. L. Xiong and R. G. Compton, *Int. J. Electrochem. Sci.*, 9 (2014) 7152.
 30. S. K. Islam and M. R. Haider, *Sensors and low power signal processing*: Springer Science & Business Media, (2009).
 31. F. Opekar and K. Štulík, *Encyclopedia of Analytical Chemistry.*, (2001).
 32. D. S. Silvester, *Analyst*, 136 (2011) 4871.
 33. N. R. C. C. o. N. S. Technologies and Applications, *Expanding the vision of sensor materials*: National Academies Press, (1995).
 34. R. d. B. J.R. Istas, L. de Temmerman, Guns, K. MeeusVerdinne, A. Ronse, P. Scokart, and M. Termonia, *European Communities.*, p. Report No. EUR 11857 EN, (1988).
 35. R. B. McCulloch, G. S. Few, G. C. Murray, and V. P. Aneja, *Environ. Pollut.*, 102 (1998) 263.
 36. Y. Li, H. Ban, and M. Yang, *Sens. Actuator B-Chem.*, 224 (2016) 449.
 37. S. Xu, K. Kan, Y. Yang, C. Jiang, J. Gao, L. Jing, P. Shen, L. Li, and K. Shi, *J. Alloys Compd.*, 618 (2015) 240.
 38. J. Deng, R. Zhang, L. Wang, Z. Lou, and T. Zhang, *Sens. Actuator B-Chem.*, 209 (2015) 449.
 39. B. Wu, L. Wang, H. Wu, K. Kan, G. Zhang, Y. Xie, Y. Tian, L. Li, and K. Shi, *Microporous Mesoporous Mater.*, 225 (2016) 154.
 40. Y. Lin, K. Kan, W. Song, G. Zhang, L. Dang, Y. Xie, P. Shen, L. Li, and K. Shi, *J. Alloys Compd.*, 639 (2015) 187.
 41. L. Dai, G. Yang, H. Zhou, Z. He, Y. Li, and L. Wang, *Sens. Actuator B-Chem.*, 224 (2016) 356.
 42. W. Meng, L. Dai, J. Zhu, Y. Li, W. Meng, H. Zhou, and L. Wang, *Electrochim. Acta*, 193 (2016) 302.
 43. X. Liang, T. Zhong, H. Guan, F. Liu, G. Lu, and B. Quan, *Sens. Actuator B-Chem.*, 136 (2009) 479.
 44. D. Schönauer, K. Wiesner, M. Fleischer, and R. Moos, *Sens. Actuator B-Chem.*, 140 (2009) 585.
 45. D. Schönauer-Kamin, M. Fleischer, and R. Moos, *Sensors (Basel)*, 13 (2013) 4760.
 46. D. Schönauer, T. Nieder, K. Wiesner, M. Fleischer, and R. Moos, *Solid State Ionics*, 192 (2011) 38.
 47. D. Schönauer-Kamin, M. Fleischer, and R. Moos, *Solid State Ionics*, 262 (2014) 270.
 48. I. Lee, B. Jung, J. Park, C. Lee, J. Hwang, and C. O. Park, *Sens. Actuator B-Chem.*, 176 (2013) 966.
 49. X. D. Li, Y. Chen, L. H. Zhou, F. Xia, and J. Z. Xiao, *Key Eng. Mater.*, (2014) 851.
 50. X. Li, C. Wang, B. Wang, Y. Yuan, J. Huang, H. Zhang, F. Xia, and J. Xiao, *Ceram. Intl.*, 42

- (2016) 2214.
51. F. Liu, R. Sun, Y. Guan, X. Cheng, H. Zhang, Y. Guan, X. Liang, P. Sun and G. Lu, *Sens. Actuator B-Chem.*, 210 (2015) 795.
 52. M. Mori, Y. Itagaki, Y. Sadaoka, S.-i. Nakagawa, M. Kida, and T. Kojima, *Sens. Actuator B-Chem.*, 191 (2014) 351.
 53. J. F. M. Oudenhoven, W. Knoben, and R. van Schaijk, *Procedia Eng.*, 120 (2015) 983.
 54. K. Murugappan, J. Lee, and D. S. Silvester, *Electrochem. Commun.*, 13 (2011) 1435.
 55. Q. Diao, F. Yang, C. Yin, J. Li, S. Yang, X. Liang, and G. Lu, *Solid State Ionics*, 225 (2012) 328.
 56. S. Cui, H. Pu, G. Lu, Z. Wen, E. C. Mattson, C. Hirschmugl, M. Gajdardziska-Josifovska, M. Weinert, and J. Chen, *ACS Appl Mater Interfaces*, 4 (2012) 4898.
 57. S. Abdulla, T. L. Mathew, and B. Pullithadathil, *Sens. Actuator B-Chem.*, 221 (2015) 1523.
 58. S. G. Bachhav and D. R. Patil, *Journal of Materials Science and Chemical Engineering*, 03 (2015) 30.
 59. Y. Guan, C. Yin, X. Cheng, X. Liang, Q. Diao, H. Zhang, and G. Lu, *Sens. Actuator B-Chem.*, 193 (2014) 501.
 60. C. Bohnke, S. Lorant, V. Gunes, J.-Y. Botquelen, and J. Breviere, *Solid State Ionics*, 262 (2014) 279.
 61. J. Kim and K. Yong, *J. Phys. Chem. C*, 115 (2011) 7218.
 62. Z. S. Hosseini, A. I. zad, and A. Mortezaali, *Sens. Actuator B-Chem.*, 207 (2015) 865.
 63. Z. S. Hosseini, A. Mortezaali, A. Irajizad, and S. Fardindoost, *J. Alloys Compd.*, 628 (2015) 222.
 64. L. Yin, D. Chen, X. Cui, L. Ge, J. Yang, L. Yu, B. Zhang, R. Zhang, and G. Shao, *Nanoscale*, 6 (2014) 13690.
 65. L. T. Lanh, T. T. Hoa, N. D. Cuong, D. Q. Khieu, D. T. Quang, N. V. Duy, N. D. Hoa, and N. V. Hieu, *J. Alloys Compd.*, 635 (2015) 265.
 66. H. Zhang, T. Zhong, R. Sun, X. Liang, and G. Lu, *RSC Adv.*, 4 (2014) 55334.
 67. C. Baker, W. Laminack, and J. L. Gole, *Sens. Actuator B-Chem.*, 212 (2015) 28.
 68. M. Asad, M. H. Sheikhi, M. Pourfath, and M. Moradi, *Sens. Actuator B-Chem.*, 210 (2015) 1.
 69. M. MalekAlaie, M. Jahangiri, A. M. Rashidi, A. HaghighiAsl, and N. Izadi, *Mater. Sci. Semicond. Process.*, 38 (2015) 93.
 70. H. Kim, C. Jin, S. Park, S. Kim, and C. Lee, *Sens. Actuator B-Chem.*, 161 (2012) 594.
 71. A. I. Ayesh, A. F. S. Abu-Hani, S. T. Mahmoud, and Y. Haik, *Sens. Actuator B-Chem.*, 231 (2016) 593.
 72. A. Gutiérrez, B. Hsia, A. Sussman, W. Mickelson, A. Zettl, C. Carraro, and R. Maboudian, *Nanoscale*, 4 (2012) 438.
 73. L. Zhou, F. Shen, X. Tian, D. Wang, T. Zhang, and W. Chen, *Nanoscale*, 5 (2013) 1564.
 74. M. M. Alaie, M. Jahangiri, A. Rashidi, A. H. Asl, and N. Izadi, *J. Ind. Eng. Chem.*, 29 (2015) 97.
 75. T. V. Cuong, V. H. Pham, J. S. Chung, E. W. Shin, D. H. Yoo, S. H. Hahn, J. S. Huh, G. H. Rue, E. J. Kim, S. H. Hur, and P. A. Kohl, *Mater. Lett.*, 64 (2010) 2479.
 76. N. Ramgir, M. Ghosh, P. Veerender, N. Datta, M. Kaur, D. Aswal, and S. K. Gupta, *Sens. Actuator B-Chem.*, 156 (2011) 875.
 77. M. Zhao, X. Wang, L. Ning, J. Jia, X. Li, and L. Cao, *Sens. Actuator B-Chem.*, 156 (2011) 588.
 78. P. Patnaik, *Handbook of environmental analysis: chemical pollutants in air, water, soil, and solid wastes*: CRC Press, (2010).
 79. J. Mohler and C. Collier, *"Handbook of Hazardous Materials,"* ed: Academic Press, (1993).
 80. Q. Diao, C. Yin, Y. Liu, J. Li, X. Gong, X. Liang, S. Yang, H. Chen, and G. Lu, *Sens. Actuator B-Chem.*, 180 (2013) 90.
 81. S. Prakash, S. Rajesh, S. K. Singh, K. Bhargava, G. Ilavazhagan, V. Vasu and C. Karunakaran,

- Talanta*, 85 (2011) 964.
82. T. Striker, V. Ramaswamy, E. N. Armstrong, P. D. Willson, E. D. Wachsman, and J. A. Ruud, *Sens. Actuator B-Chem.*, 181 (2013) 312.
 83. I. Romanytsia, J.-P. Viricelle, P. Vernoux, and C. Pijolat, *Sens. Actuator B-Chem.*, 207 (2015) 391.
 84. D. Yan, M. Hu, S. Li, J. Liang, Y. Wu, and S. Ma, *Electrochim Acta*, 115 (2014) 297.
 85. G. Paściak, W. Mielcarek, K. Prociów, and J. Warycha, *Ceram. Int.*, 40 (2014) 12783.
 86. J. Gao, J.P. Viricelle, C. Pijolat, P. Breuil, P. Vernoux, A. Boreave, and A. G. Fendler, *Sens. Actuator B-Chem.*, 154 (2011) 106.
 87. C. López-Gándara, J. M. Fernández-Sanjuán, F. M. Ramos, and A. Cirera, *Solid State Ionics*, 184 (2011) 83.
 88. M. M. Shahid, P. Rameshkumar, A. Pandikumar, H. N. Lim, Y. H. Ng, and N. M. Huang, *J. Mater. Chem. A*, 3 (2015) 14458.
 89. H. K. Gatty, S. Leijonmarck, M. Antelius, G. Stemme, and N. Roxhed, *Sens. Actuator B-Chem.*, 209 (2015) 639.
 90. C. W. Chang, G. Maduraiveeran, J. C. Xu, G. W. Hunter, and P. K. Dutta, *Sens. Actuator B-Chem.*, 204 (2014) 183.
 91. L. Wang, Y. Wang, L. Dai, Y. Li, J. Zhu, and H. Zhou, *J. Alloys Compd.*, 583 (2014) 361.
 92. Y. Chen and J. Xiao, *Sens. Actuator B-Chem.*, 192 (2014) 730.
 93. Z. Zheng, H. Ren, I. VonWald, and M. E. Meyerhoff, *Anal Chim Acta*, 887 (2015) 186.
 94. L. S. Berisha, A. Maloku, T. Arbnesi, and K. Kalcher, *Sensors & Transducers.*, 184 (2015) 159.
 95. L. Wang, B. Han, Z. Wang, L. Dai, H. Zhou, Y. Li, and H. Wang, *Sens. Actuator B-Chem.*, 207 (2015) 791.
 96. X. Li, C. Wang, J. Huang, Y. Yuan, B. Wang, H. Zhang, F. Xia, and J. Xiao, *Ceram. Int.*, 42 (2016) 9363.
 97. F. Liu, X. Yang, B. Wang, Y. Guan, X. Liang, P. Sun, and G. Lu, *Sens. Actuator B-Chem.*, 229 (2016) 200.
 98. S. Ghashghaie, S. S. S. Ahmadi, B. Raissi, R. Riahifar, M. S. Yaghmaee, and M. Javaheri, *Mater Lett.*, 141 (2015) 23.
 99. J. Zosel, G. Schiffel, F. Gerlach, K. Ahlborn, U. Sasum, V. Vashook, and U. Guth, *Solid State Ionics*, 177 (2006) 2301.
 100. A. Kalyakin, J. Lyagaeva, D. Medvedev, A. Volkov, A. Demin, and P. Tsiakaras, *Sens. Actuator B-Chem.*, 225 (2016) 446.
 101. H. G. Moon, Y. S. Shim, D. H. Kim, H. Y. Jeong, M. Jeong, J. Y. Jung, S. M. Han, J. K. Kim, J. S. Kim, H.H. Park, J. H. Lee, H. L. Tuller, S. J. Yoon, and H. W. Jang, *Sci. Rep.*, 2 (2012).